Dalton Transactions

ROYAL SOCIETY OF CHEMISTRY

FRONTIER

View Article Online
View Journal | View Issue

Cite this: *Dalton Trans.*, 2023, **52**, 17666

Redox-active ligands – a viable route to reactive main group metal compounds

Glen G. Briand

Received 20th September 2023,
Accepted 16th November 2023

DOI: 10.1039/d3dt03100d

rsc.li/dalton

Anionic redox-active ligands such as *o*-amidophenolates, catecholates, dithiolenes, 1,2-benzendithiolates, 2-amidobenzenethiolates, reduced α-diimines, ferrocenyl and porphyrinates are capable of reversible oxidation and thus have the ability to act as sources of electrons for metal centres. These and other non-innocent ligands have been employed in coordination complexes of base transition metals to influence their redox chemistry and afford compounds with useful catalytic, optical, magnetic and conducting properties. Despite the focus in contemporary main group chemistry on designing reactive compounds with potential catalytic activity, comparatively few studies exploring the chemistry of main group metal complexes incorporating redox-active ligands have been reported. This article highlights relevant chemical reactivity and electrochemical studies that probe the oxidation/reduction of main group metal compounds possessing redox-active ligands and comments on the prospects for this relatively untapped avenue of research.

Introduction

A current focus of main group chemistry is the mimicry of the catalytic behavior of organometallic complexes of precious transition metals for organic transformations important to the fine chemicals and pharmaceuticals industries.[1–4] Specifically, these metals are particularly suited for catalyzing coupling reactions as they often favour two-electron redox changes thus allowing for "oxidative addition" of substrates, rearrangement of ligands and subsequent "reductive elimination" of products. Heavy main group metals such as indium and bismuth are desirable alternatives to these due to their lower toxicity compared to these precious transition metals and other heavy main metals (*e.g.* Tl, Sn, Pb, Sb), lower cost and high Lewis acidity due to their large atomic radii. However, these metals are predominantly stable in one oxidation state and do not typically undergo reversible oxidation reactions. Indium is most stable in the +3 oxidation state, though mononuclear indium(I) species which feature a reactive valence lone pair of electrons may be isolated. Chemical oxidation of these compounds to indium(III) has been demonstrated, but the corresponding reduction reactions have not. Bismuth is also predominantly stable in the +3 state but possesses a lone pair of valence electrons that is relatively non-reactive due to the inert pair effect. Bismuth(V) compounds may be isolated with the appropriate choice of ligand and, more recently, Cornella *et al.* have employed a ligand framework that permits chemical oxidation of bismuth(III) to bismuth(V) species, followed by subsequent reductive elimination of products. This demonstrates the use of an organobismuth compound capable of a III/V redox couple in a catalytic cycle.[5–7]

An alternative approach to designing heavy main group metal compounds capable of redox chemistry is through use of non-innocent "redox-active" ligands.[8] Anionic ligands such as *o*-amidophenolates (AP), catecholates (Cat), dithiolenes (mnt), 1,2-benzenedithiolates (tdt), 2-amidothiophenolates (abt), reduced α-diimides (DAB, BIAN) and ferrocenyl ligands (Fc) are capable of reversible one-electron oxidation, while porphyrins (Por) are capable of two-electron processes (Fig. 1). Therefore, complexation with these ligands allows for potentially reversible oxidation of organometallic complexes possessing metal centres with inaccessible or no valence electrons. These ligands have found use in the synthesis of base transition metal complexes with useful catalytic properties by suppressing favourable one-electron redox processes and facilitating two-electron processes.[9–15] They have also been employed in preparing complexes with a variety of interesting optical, magnetic and conducting properties and applications in new generations of optoelectronic devices.[16]

Chemical reactivity and electrochemistry

Heavy main group metal complexes of these redox-active ligands have been known for more than 50 years.[17,18] Of the comparatively few reports of these complexes *versus* those of base transition metals, the majority are limited to synthetic or structural studies. As an illustration of the current state of the

Department of Chemistry and Biochemistry, Mount Allison University, Sackville, New Brunswick E4L 1G8, Canada. E-mail: gbriand@mta.ca

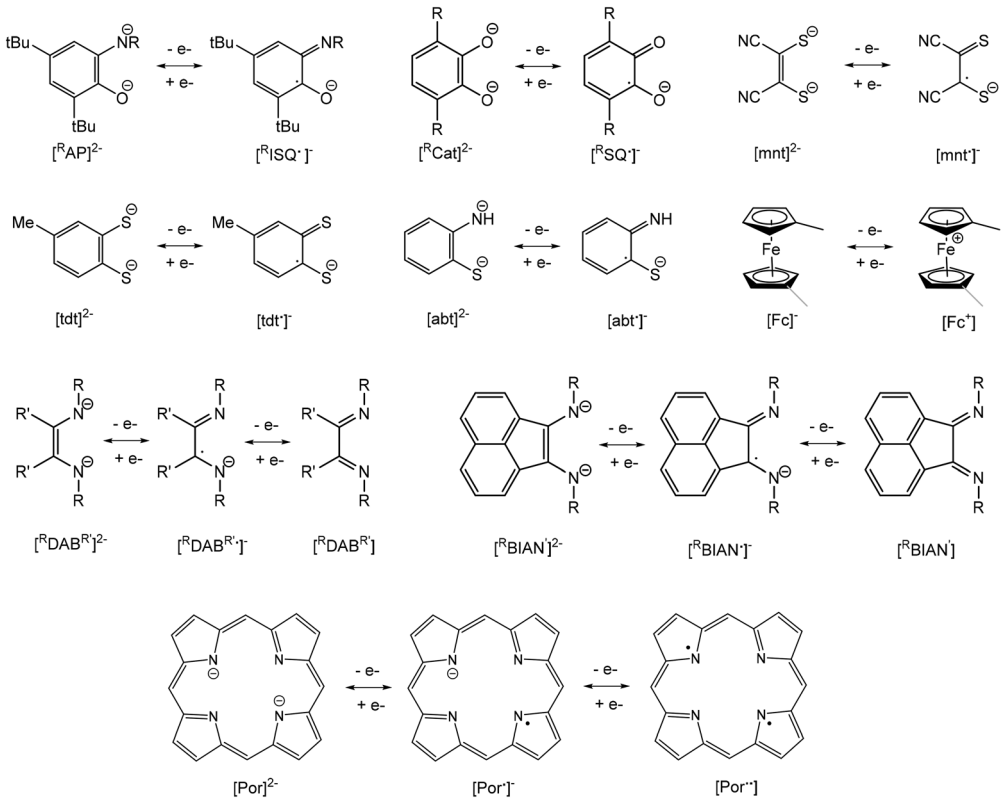

Fig. 1 Redox couples of redox-active ligands capable of acting as electron reservoirs: *o*-amidophenolate (AP)/*o*-iminosemiquinone (ISQ), catecholate (Cat)/*o*-semiquinone (SQ), maleonirileditholate (mnt), 3,4-toluenedithiolate (tdt), 2-amidobenzenethiolate (abt), ferrocenyl (Fc), 1,4-diaza-1,3-butabiene (DAB), 1,2-bis(imino)acenaphthene (BIAN) and porphyrinato (Por).

field, the following highlights relevant chemical reactivity or electrochemical studies that report oxidation/reduction of main group metal compounds.

o-Amidophenolates (AP)

Structural drawings of select main group metal *o*-amidophenolate complexes are found in Fig. 2. Group 13 complexes of *o*-amidophenolate have been studied extensively by Piskunov and have been recently reviewed.[19] The reaction of the heteroleptic complexes (^{Dipp}AP)GaX (X = Me, I) (Dipp = 2,6-diisopropylphenyl) with single-electron oxidants (I_2, O_2, $HgCl_2$, $HgBr_2$, TMUDS = tetramethylthiuram disulfide) results in oxidation of the $[^{Dipp}AP]^{2-}$ ligand and formation of a monoradical species, as confirmed by EPR studies, which spontaneously symmetrize to a paramagnetic neutral biradical species (^{Dipp}ISQ$^{\bullet}$)$_2$GaX/Y.[20] Attempted synthesis of (^{Dipp}AP)InI *via* metathesis reaction resulted in oxidation of the $(^{Dipp}AP)^{2-}$ ligand and formation of the diradical species (^{Dipp}ISQ$^{\bullet}$)$_2$InI.[21] However, the reduced ligand complex (^{Dipp}AP)InI(tmeda) (**1**) (tmeda = *N*,*N*,*N*′,*N*′-tetramethylethylenediamine) could be isolated in the presence of the coordinating tmeda ligand.[22] Reaction of **1** with oxidizing agents I_2 or $HgCl_2$ resulted in single oxidation of the $(^{Dipp}AP)^{2-}$ ligand and isolation of (^{Dipp}ISQ$^{\bullet}$)InX_2(tmeda) (X = I or Cl, respectively).[23] The stability of these complexes *versus* the corresponding gallium complexes is attributed to the coordination of the tmeda ligand to the metal centre. Alternatively, reaction of **1** with O_2 or TMTUDS (tetramethylthiuramedisulfide) led to disproportionation and formation of the bis-ligand species (^{Dipp}ISQ$^{\bullet}$)$_2$InX (X = I or S_2CNMe_2, respectively), the latter of which proceeds through the expected (^{Dipp}ISQ$^{\bullet}$)InI(S_2CNMe_2)(tmeda) intermediate as determined by EPR spectroscopy. Similar reactivity was observed for $[(^{Dipp}AP)InEt]_2$. Oxidation of the homoleptic monoanion of $[(DME)_3Na]^+[(^{Dipp}AP)_2In]^-$ (**2**) (DME = dimethoxyethane) with Hg_2X_2 (X = Cl, Br) gives the corresponding 2-electron oxidized products (^{Dipp}ISQ$^{\bullet}$)$_2$InX.[24] Attempted activation of RI (R = Me, Et) with **2** in thf proceeds slowly at room temperature and more quickly at reflux temperatures to give diamagnetic **3**.[25] The reaction results in the formal addition of the alkyl cation group to the $(^{Dipp}AP)^{2-}$ ligand to give $(^{Dipp}RAP)^-$ and addition of the iodide anion to the indium centre. Activation of allyl halides (AllX, X = Cl, Br, I) with $[(thf)_2Na(^{Dipp}AP)_2Ga]$ yields analogous products to **3**, with the reaction of AllI completed in a few hours and that with AllCl requiring more than two weeks.[26] Attempts to isolate (^{Dma}ISQ$^{\bullet}$)$_3$Ga ($H_2{}^{Dma}$Ap = 2-(3,5-dimethoxyanilino)-4,6-di-*tert*-butylphenol) from the reaction of $GaCl_3$ and $H_2{}^{Dma}$Ap in the presence of Et_3N resulted in the formation of **4**, which features C–H bond activation of the $(^{Dma}AP^{2)-}$ ligand and the formation of new C–N bonds, presumably as a result of the

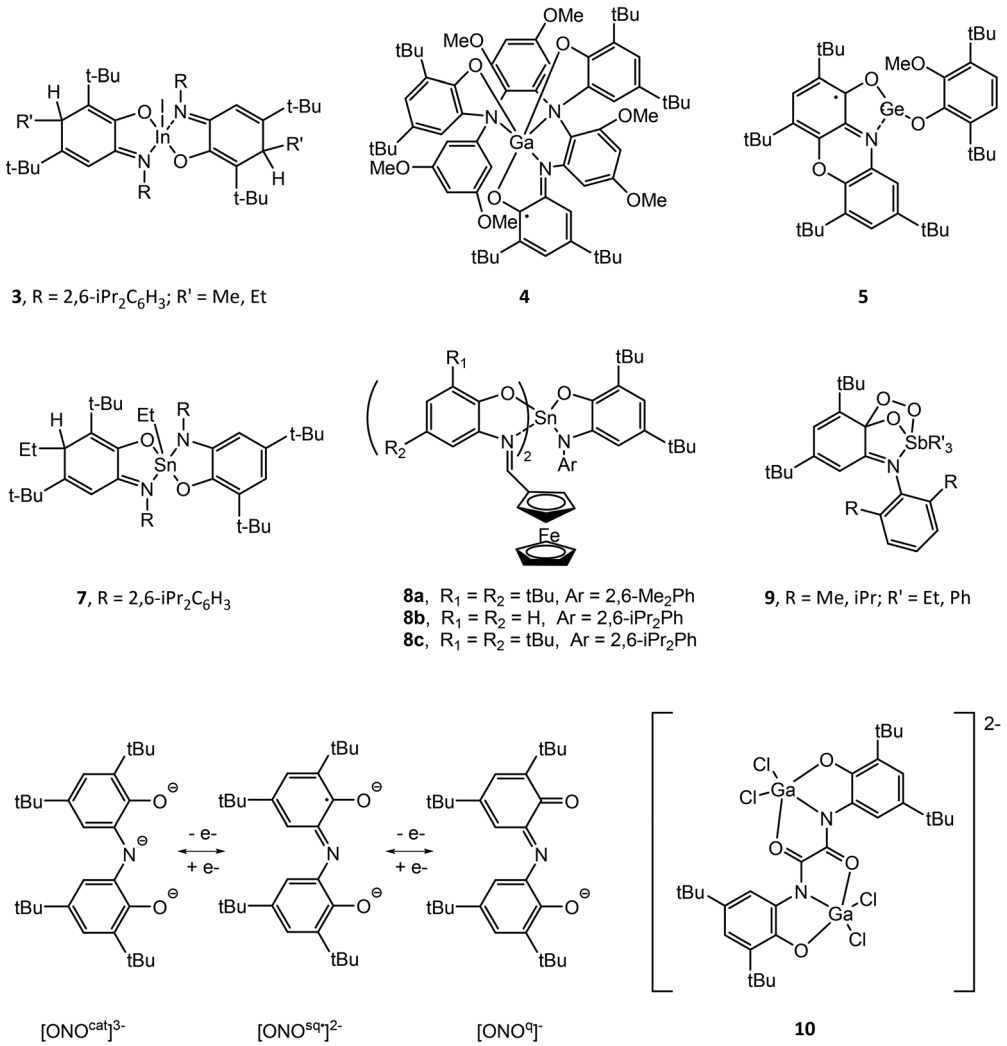

Fig. 2 Structural drawings of select main group metal *o*-amidophenolate (AP) compounds and ligands.

absence of *ortho*-substituents in the *N*-[3,5-$(MeO)_2C_6H_3$] group.[27]

(^{Phenox}AP)Ge^{II} (^{Phenox}AP = 2,4,6,8-tetra-*tert*-butylphenoxazin-1-one) reacts with the one-electron oxidant 3,6-di-*tert*-butyl-2-methoxyphenoxyl radical (RO$^{\bullet}$) to afford (^{Phenox}ISQ$^{\bullet}$)Ge^{II}(OR) (**5**), in which the (^{Phenox}AP)$^{2-}$ ligand *versus* the Ge^{II} centre is oxidized.[28] Cyclic voltammetry (CV) studies of (^{R}AP)Ge^{II} (R = Ad (**6a**), Ph (**6b**), *t*Bu (**6c**)) show a single irreversible oxidation wave for **6a** and **6c** and a single quasi-reversible wave for **6b**. Chemical oxidation of **6a–c** with the 3,6-di-*tert*-butyl-2-ethoxyphenoxy radical allowed for detection of the **6a**$^{\bullet+}$ radical only by EPR spectroscopy.[29] Oxidation of (^{R}AP)Sn^{II} (R = Ad, *t*Bu) with TMTDS results in oxidation of Sn^{II} and formation of (^{R}AP)$Sn^{IV}(S_2CNMe_2)_2$.[30]

The homoleptic compound (^{tBu}AP)$_2Sn^{IV}$ has been shown to display redox isomerism with the tin(II) electromeric form (^{tBu}ISQ$^{\bullet}$)$_2Sn^{II}$ in non-polar solvents, as determined by magnetochemistry, EPR, UV-visible spectroscopy and Mössbauer spectroscopy.[31] The interconversion can be quenched through addition of a strong donor solvent such as pyridine, resulting in the octahedral compound (^{tBu}AP)$_2Sn^{IV}$(py)$_2$. Reaction of the six-coordinate complex (^{Dipp}AP)(^{Dipp}ISQ$^{\bullet}$)$_2Sn^{IV}$ with air oxygen produces [(^{Dipp}AP)(^{Dipp}ISQ$^{\bullet}$)Sn]$_2$O and (^{Dipp}ISQ$^{\bullet}$)$_2$Sn(OH)$_2$ containing μ-oxo- and hydroxo- ligands, respectively.[32] Oxidation of [(^{Dipp}AP)Pb^{II}]$_2$ with Hg_2Br_2 affords the radical species [(^{Dipp}ISQ$^{\bullet}$)Pb^{II}Br] as detected by EPR spectroscopy.[33]

Reaction of (^{Dipp}AP)$Sn^{IV}Ph_2$ with dioxygen yields the ligand oxidized species (^{Dipp}ISQ$^{\bullet}$)$_2Sn^{IV}Ph_2$ and Ph_2SnO, while oxidation with sulfur yields (^{Dipp}AP)(^{Dipp}ISQ$^{\bullet}$)SnPh and (Ph_3Sn)S.[34] Alternatively, reaction of [(^{Dipp}AP)$Sn^{IV}Et_2$(thf)] with dioxygen or sulfur yields (^{Dipp}ISQ$^{\bullet}$)$_2Sn^{IV}Et_2$, which spontaneously undergoes alkyl elimination to give (^{Dipp}AP)(^{Dipp}ISQ$^{\bullet}$)Sn^{IV}Et, (^{Dipp}AP)(^{Dipp}EtAp)Sn^{IV}Et (**7**) and Et_2SnE (E = O, S). Reaction of (^{Dipp}AP)$Sn^{IV}t$Bu$_2$ with allylhalides AllX (X = Cl, Br, I) results in alkyl transfer to the ring carbon and a C–C bond formation similar to that observed for **7**. Alternatively, reaction of (^{Dipp}AP)Sn^{II} with AllX results in oxidation of the tin centre and formation of (^{Dipp}AP)Sn(All)X followed by disproportionation to

(^{Dipp}AP)$_2$Sn and a similar alkyl transfer to the ring carbon atoms.[35] (^{Dipp}AP)Sn^{II} reacts with TMTD (tetramethylthiuram disulfide) to give oxidation at tin and isolation of (^{Dipp}AP)Sn^{IV}(S_2CNMe_2)$_2$, while reaction with ethoxy-3,6-di-*tert*-butylphenoxy radical (OR$^{\bullet}$) results in formation of (^{Dipp}ISQ$^{\bullet}$)Sn^{II}(OR), as determined by EPR spectroscopy at low temperature.[36]

A series of tin(IV) complexes (^{Dipp}AP)Sn^{IV}(IPFc)$_2$ (IPFc = 2-(ferrocenylmethyleneamino)phenolate) (**8a–c**) containing both *o*-amidophenolate and ferrocenyl ligands have been studied by CV.[37] Generally, these complexes show four quasi-reversible oxidations assigned to oxidation of (^{Dipp}AP)$^{2-}$ to (^{Dipp}ISQ$^{\bullet}$)$^{-}$ to neutral *o*-iminoquinone at lower potentials followed by the separate oxidation of each (IPFc) to (IPFc^{+}) at higher potentials. Chemical oxidation of **8b** and **8c** with silver triflate and characterization of the resulting products by EPR supported the assignment of the first oxidation and the formation of [(^{Dipp}ISQ$^{\bullet}$)Sn^{IV}(IP-Fc)$_2$]$^{+}$ (**8b**$^{\bullet+}$ and **8c**$^{\bullet+}$).

The antimony compounds (^{R}AP)Sb^{V}R$_3$ (R = Dmp, Dipp; R′ = Et, Ph), which are prepared from the oxidative addition of neutral *o*-iminobenzoquinone and R′$_3$Sb^{III}, have been shown to reversibly bond dioxygen.[38–42] The compounds are air stable but bind molecular oxygen in solution to yield (^{R}AP)(O$_2$)SbR′$_3$ (**9**), which features a trioxastibolane ring as determined by X-ray crystallography. Moderate heating of solutions of **9** lead to elimination of O$_2$ and isolation of (^{R}AP)SbR′$_3$. The proposed mechanism involves oxidation of the (^{R}AP)$^{2-}$ ligand and formation of a [(^{R}ISQ$^{\bullet}$)Sb^{V}R′$_3$]$^{+}$[O$_2^{\bullet}$]$^{-}$ ion pair as an initial step.

3,5-di-*tert*-Butyl-1,2-quinone-1-(2-hydroxy-3,5-di-*tert*-butylphenyl)imine (ONO) ligands can exist in three anionic oxidation states (Fig. 2).[43] The complexes (ONO^{q})Al(AcacPh$_2$)Cl (AcacPh$_2^{-}$ = diphenylacetylacetonate) and (ONO^{q})Al(QuinO)Cl (QuinO^{-} = 8-oxyquinoline) were reduced with KC$_8$ to undergo a single-electron reduction in the presence of pyridine to give [(ONO$^{sq\bullet}$)Al(AcacPh$_2$)(py)]$^{-}$ and [(ONO$^{sq\bullet}$)Al(QuinO)(py)]$^{-}$ monoradicals.[44] Alternatively, oxidation of (HONO^{cat})AlCl(OEt$_2$) with tetrachloro-1,2-quinone (*o*-O$_2$C$_6$Cl$_4$), 9,10-phenanthrenequinone (*o*-O$_2$C$_{14}$H$_8$) or pyrene-4,5-dione (*o*-O$_2$C$_{16}$H$_8$) in the presence of pyridine results in expulsion of HCl and the formation of (ONO$^{sq\bullet}$)Al(*o*-O$_2$C$_6$Cl$_4^{\bullet}$)(py), (ONO$^{sq\bullet}$)Al(*o*-O$_2$C$_{14}$H$_8^{\bullet}$)(py) and (ONO$^{sq\bullet}$)Al(*o*-O$_2$C$_{16}$H$_8^{\bullet}$)(py), respectively, which possess two redox-active ligands. The assignment of the radical semiquinone redox state of the ligands was determined using X-ray crystallography, UV-vis-NIR spectroscopy and magnetic measurements. The [N(*n*Bu)$_4$]$^{+}$ salt of the binuclear dianionic gallium complex [(bbpo)(GaCl$_2$)$_2$]$^{2-}$ (**10**) (H$_4$bbpo = 1,2-bis(3,5-di-*tert*-butyl-2-hydroxyphenyl)oxamine) has been studied by CV and exhibits two ligand-centred reversible one-electron oxidation waves.[45] Magnetic measurements show two uncoupled (*o*-iminobenzosemiquinonate)gallium(III) units at room temperature.

Catecholates (Cat)

Structural drawings of select main group metal catecholate complexes are found in Fig. 3. The reaction of [(^{tBu}Cat)InI(thf)]$_2$ (**11**) and [(^{tBu}Cat)InMe]$_3$ (**12**) and with oxidizing agents was studied by EPR spectroscopy.[46] Reaction of **11** with one equivalent of I$_2$ in thf gave (^{tBu}SQ$^{\bullet}$)InI$_2$(thf) (**13**), which features the monooxidized (^{tBu}SQ$^{\bullet}$)$^{-}$ ligand. Dissolution of **13** in diethyl ether lead to spontaneously disproportionation to (^{tBu}SQ$^{\bullet}$)$_2$InI and InI$_3$. Alternatively, dissolution of **13** in non-coordinating toluene or hexane solvent resulted in formation of the homoleptic triradical (^{tBu}SQ$^{\bullet}$)$_3$In (**14**). This compound undergoes ligand exchange with tmeda to eliminate neutral *o*-benzoquinone and form (^{tBu}Cat)(^{tBu}SQ$^{\bullet}$)In(tmeda) *via* intramolecular electron transfer between (^{tBu}SQ$^{\bullet}$)$^{-}$ ligands. Reaction of [(^{tBu}Cat)InMe]$_3$ (**12**) with 1.5 equivalents of I$_2$ gave (^{tBu}SQ$^{\bullet}$)InMeI, which spontaneously disproportionates to (^{tBu}SQ$^{\bullet}$)$_3$In (**14**), MeInI$_2$ and Me$_2$InI. This is presumably due to the weak coordination of thf in (^{tBu}SQ$^{\bullet}$)InMeI *versus* (^{tBu}SQ$^{\bullet}$)InI$_2$(thf) (**13**). Similar reactivity is observed for **11** with TMTUDS to give the radical species (^{tBu}SQ$^{\bullet}$)InI(TMTUDS), which is stable in thf but further reacts in non-coordinating solvent to give (^{tBu}SQ$^{\bullet}$)$_3$In (**14**). An analogous result is observed for the corresponding reaction of **12** and TMTUDS, though the product (^{tBu}SQ$^{\bullet}$)InMe(TMTUDS) slowly disproportionates in thf to

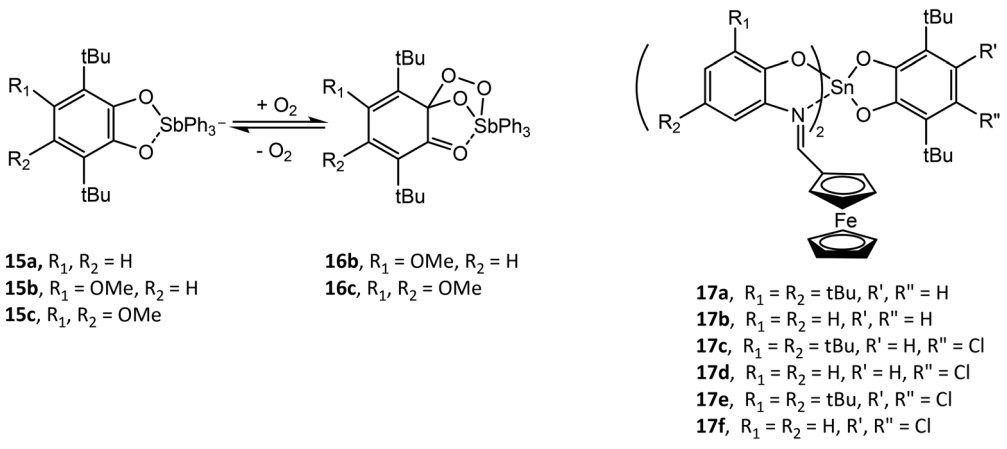

15a, R$_1$, R$_2$ = H
15b, R$_1$ = OMe, R$_2$ = H
15c, R$_1$, R$_2$ = OMe

16b, R$_1$ = OMe, R$_2$ = H
16c, R$_1$, R$_2$ = OMe

17a, R$_1$ = R$_2$ = tBu, R', R" = H
17b, R$_1$ = R$_2$ = H, R', R" = H
17c, R$_1$ = R$_2$ = tBu, R' = H, R" = Cl
17d, R$_1$ = R$_2$ = H, R' = H, R" = Cl
17e, R$_1$ = R$_2$ = tBu, R', R" = Cl
17f, R$_1$ = R$_2$ = H, R', R" = Cl

Fig. 3 Structural drawings of select main group metal catecholate (Cat) compounds and reaction schemes.

($^{t\text{Bu}}$SQ$^{\bullet}$)$_2$InMe. The products of these reactions depend on the reaction conditions, notably the solvent.

As with ($^{\text{Dipp}}$AP)Sn$^{\text{II}}$, ($^{t\text{Bu}}$Cat)Sn$^{\text{II}}$ also reacts with TMTD to give oxidation at Sn$^{\text{II}}$ and isolation of ($^{t\text{Bu}}$Cat)Sn$^{\text{IV}}$(S_2CNMe_2)$_2$, while reaction with ethoxy-3,6-di-*tert*-butylphenoxy radical (OR$^{\bullet}$) results in oxidation of the catecholate ligand and formation of ($^{t\text{Bu}}$SQ$^{\bullet}$)Sn$^{\text{II}}$(OR), as determined by EPR spectroscopy at low temperature.[36]

Analogous to ($^{\text{R}}$AP)Sb$^{\text{V}}$R′$_3$ (R = Dmp, Dipp; R′ = Et, Ph), a series of antimony catecholate compounds ($^{\text{R}}$Cat)Sb$^{\text{V}}$R′$_3$ (R′ = Et, Ph) (**15**) is prepared from the oxidative addition of neutral *o*-benzoquinone and R′$_3$Sb$^{\text{III}}$ and reversibly bonds dioxygen to give ($^{\text{R}}$Cat)(O_2)SbR′$_3$ (**16**).[38,42,47–49] In addition to computational studies on the effect of the electronic and steric properties of the catecholate or *o*-amidophenolate ligand on reactivity, it has been demonstrated experimentally that the redox potential of the ligand is crucial in allowing or forbidding the binding process. For example, (4,5-(MeO)$_2$-$^{t\text{Bu}}$Cat)SbPh$_3$ (**15b**) (4,5-(MeO)$_2$-$^{t\text{Bu}}$Cat = 4,5-dimethoxy-3,6-di-*tert*-butyl-catecholato) and (4-MeO-$^{t\text{Bu}}$Cat)SbPh$_3$ (**15c**) (4-MeO-$^{t\text{Bu}}$Cat = 4-methoxy-3,6-di-*tert*-butyl-catecholato) undergo reversible addition of dioxygen while ($^{t\text{Bu}}$Cat)SbPh$_3$ (**15a**) does not. This is a result of the electron donor ability of the methoxy group, which allows the catechol ligand to be more easily oxidized. (4,5-Cat)SbR′$_3$ (4,5-Cat = 4,5-(1,1,4,4-tetramethyl-butane-1,4-diyl)-catecholato; R′ = Et, Ph) and [Ph_4Sb]$^+$[(4,5-Cat)$_2$SbPh$_2$]$^-$ have been studied by CV. (4,5-Cat)SbPh$_3$ undergoes one reversible one-electron ligand oxidation to give [(4,5-SQ$^{\bullet}$)SbPh$_3$]$^+$ and a second irreversible one-electron ligand oxidation as a result of dissociation of neutral *o*-benzoquinone. Alternatively, (4,5-Cat)SbEt$_3$ undergoes two irreversible one-electron oxidations, while [(4,5-Cat)$_2$SbPh$_2$]$^-$ undergoes two reversible one-electron ligand oxidations to give [(4,5-Cat)(4,5-SQ$^{\bullet}$)SbPh$_2$] and [(4,5-SQ$^{\bullet}$)$_2$SbPh$_2$]$^+$.[48]

Similar to the *o*-amidophenolate (AP)Sn$^{\text{IV}}$(IP-Fc)$_2$ compounds **8a–c**, a series of tin(IV) complexes (Cat)Sn$^{\text{IV}}$(IPFc)$_2$ (**17a–f**) containing both catecholate and ferrocenyl ligands have been studied by CV.[37] The first two oxidations of **17a–f** are similar, with oxidation of the catecholate ligand to give [(SQ$^{\bullet}$)Sn$^{\text{IV}}$(IP-Fc)$_2$]$^+$, followed by oxidation of the IPFc ligand to give [(SQ$^{\bullet}$)Sn$^{\text{IV}}$(IPFc)(IPFc$^+$)$_2$]$^{2+}$. Compounds **17a**, **17c** and **17d** then undergo an intramolecular electron transfer to give [(Q)Sn$^{\text{IV}}$(IPFc)$_2$]$^{2+}$ (Q = *o*-benzoquinone) followed by spontaneous decoordination of the neutral *o*-benzoquinone ligand to give [Sn$^{\text{IV}}$(IPFc)$_2$]$^{2+}$. For compound **17b** and **17e**, a third oxidation wave is assigned to further oxidation of the (SQ$^{\bullet}$)$^-$ ligand, which is followed by decoordination of the neutral *o*-benzoquinone ligand to give [Sn$^{\text{IV}}$(IPFc)(IPFc$^+$)]$^{3+}$. Chemical oxidation of **17a** and **17d** with silver triflate and characterization of the resulting products by EPR supported the assignment of the first oxidation and the formation of [(SQ$^{\bullet}$)Sn(IPFc)$_2$]$^+$.

α-Diimines – 1,4-diaza-1,3-butabienes (DAB) and 1,2-bis (imino)acenaphthenes (BIAN)

Structural drawings of select main group metal complexes with reduced α-diimine ligands are found in Fig. 4. The reactivity of ($^{\text{R}}$DAB$^{\text{R}'}$)M$^{\text{II}}$–M$^{\text{II}}$($^{\text{R}}$DAB$^{\text{R}'}$) and ($^{\text{R}}$BIAN)M$^{\text{II}}$–M$^{\text{II}}$($^{\text{R}}$BIAN) (M = Al, Ga) complexes has been studied and exhibit insertion reactions into the M–M bond to afford M$^{\text{III}}$ species. For example ($^{\text{Dipp}}$DAB$^{\text{Me}}$)Al$^{\text{II}}$–Al$^{\text{II}}$($^{\text{Dipp}}$DAB$^{\text{Me}}$) (**18**) reacts with symmetric and asymmetric azo compounds to form ($^{\text{Dipp}}$DAB$^{\text{Me}\bullet}$)Al$^{\text{III}}$(μ_2-NPh)(μ_2-NAr)Al$^{\text{III}}$($^{\text{Dipp}}$DAB$^{\text{Me}\bullet}$) (**19a–c**) (Ar = Ph, *p*-MeOC_6H_4,

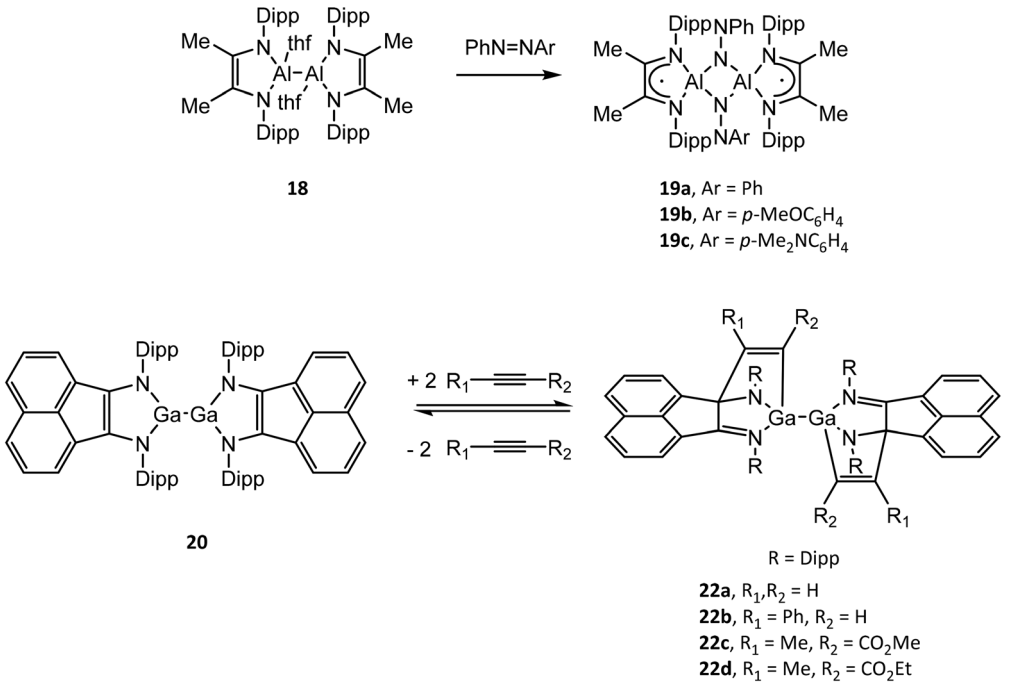

Fig. 4 Structural drawings of select reduced α-diimine (DAB, BIAN) ligand main group metal compounds and reaction schemes.

p-$Me_2NC_6H_4$) *via* oxidation of **18** and reduction of the N=N bond.[50] Further, compound **19a–c** could be reduced with Na give to the dianionic ligand complex $[(^{Dipp}DAB^{Me})Al^{III}(\mu_2\text{-NPh})(\mu_2\text{-NAr})Al^{III}(^{Dipp}DAB^{Me})]^{2-}$. $(^{Dipp}BIAN)Ga^{II}$–$Ga^{II}(^{Dipp}BIAN)$ (**20**) reacts with oxidizing agents $(SCH_2Ph)_2$, $Me_2N(S)CS$–$SC(S)NMe_2$ and I_2 to afford $(^{Dipp}BIAN^{\bullet})Ga^{III}(SCH_2Ph)_2$, $(^{Dipp}BIAN)Ga^{III}(S_2CNMe_2)$ and $(^{Dipp}BIAN^{\bullet})Ga^{III}$–$Ga^{III}(^{Dipp}BIAN^{\bullet})$ (**21**), respectively.[51,52] Compound **21** reversibly dissociates in pyridine solution to give $(^{Dipp}BIAN)Ga^{III}I(py)$. The reversible addition of alkynes to **20**, which involves direct bonding of the ^{Dipp}BIAN ligand with the substrate (**22a–d**), was exploited to facilitate the catalytic hydroamination and hydroarylation of phenylacetylene with anilines.[53,54]

Reaction of $^{Mes}DAB^{Me}$ (Mes = 2,4,6-trimethylphenyl) with $In^{I}OTf$ lead to formation of the adduct $(^{Mes}DAB^{Me})In^{I}(OTf)$, while a similar reaction with less-electron-rich $^{Mes}DAB^{H}$ resulted in formation of the reduced ligand diindane species $[(^{Mes}DAB^{H\bullet})In^{II}(OTf)]_2$ (**23**).[55] Compound **23** displays C–C coupling of the radical $[^{Mes}DAB^{H\bullet}]^-$ ligands in the solid-state. Similarly, the 3 : 2 reaction of $^{Dipp}DAB^{H}$ and $In^{I}Cl$ resulted in formation of the paramagnetic diindane $[(^{Dipp}DAB^{H\bullet})In^{II}Cl]_2$ (**24**).[56] Solution EPR data confirms the presence of a ligand based radical in both **23** and **24**. $(^{Dipp}DAB^{H\bullet})In^{III}Cl_2(thf)$ is formed in low yield from a disproportionation reaction of $(^{Dipp}DAB^{H})Li_2$ and $In^{I}Cl$, which also affords indium metal and neutral $^{Dipp}DAB^{H}$ as byproducts.[57] Reactions of $^{R}DAB^{H}$ (R = (*S*) methylbenzyl, (*R*) 1′-chlorobutan-2′-yl, (*S*,*S*) 1′-chloro-1′-phenylpropan-2′-yl or di-*tert*-butyl) with MCl_3 (M = Al, In) in acetonitrile afford $(^{R}DAB^{H})MCl_3$ adducts. The $(^{R}DAB^{H})InCl_3$ adducts slowly decompose to 1,3-dialkyl-imidazolium and alkylammonium tetrachloroindate in thf solution.[58] CV scans of the adduct $(^{pBP}BIAN)InCl_3$ (*p*BP = *p*-bromophenyl) shows two quasi-reversible reduction waves assigned to reduction of the In^{III} centre to In^{I}, with subsequent reduction waves assigned to reduction of the ^{pBP}BIAN ligand.[59] The adducts $(^{R}BIAN)InCl_3$ (R = 2,6-diisopropylphenyl (**25**), 2,6-dimethylphenyl and *p*-nitrophenyl) showed four irreversible reduction waves, likely due to the loss of Cl^- ligands during reduction of the complex.[60] Data suggested that mild reducing agents with potentials between −1.0 and −2.0 V can be used to reduce these complexes. Reduction of **25** with magnesium anthracene resulted in formation of reduced $(^{Dipp}BIAN)H_2$ and indium metal, while reduction of $(^{pMP}\text{-}BIAN)_2InCl_2[InCl_4]$ (*p*MP = *p*-methoxyphenyl) with Cp_2Co also resulted in formation of reduced $(^{pMP}\text{-}BIAN)H_2$ ligand.

$SnCl_2$ may be reacted with ^{Dipp}BIAN to afford the adduct $(^{Dipp}BIAN)Sn^{II}Cl_2$, while the monoanionic ligand complex $(^{Dipp}BIAN^{\bullet})Sn^{II}Cl$ may be prepared from ^{Dipp}BIAN and a five-fold excess of $SnCl_2$ and KC_8.[61] Reaction of ^{Dipp}BIAN with one equivalents of $SnCl_2$ and two equivalents of KC_8 in the presence of one equivalent of $[CpFe(CO)_2]_2$ gives the dianionic ligand complex $(^{Dipp}BIAN)Sn^{II}$.

It has been shown that the reaction of $Pn^{I}Cl$ (Pn = P, As), generated *in situ* from $PnCl_3$ and $SnCl_2$ as reductant, with ^{Dipp}BIAN results in formation of N-heterocyclicphosphinium and -arsinium cations $[(^{Dipp}BIAN)Pn^{III}][SnCl_5\cdot thf]$.[62] The Pn^{III} oxidation state was confirmed by ^{31}P NMR and bond distances and angles elucidated from X-ray crystal structures. Similarly, reaction of $P^{I}Br$, generated *in situ* from PBr_3 and cyclohexene, with $(^{R}DAB^{H})$ (R = Mes, Dipp) or $(^{R}BIAN)$ (R = Mes, Dipp) affords $(^{R}DAB^{H})PBr$ or $(^{R}BIAN)PBr$ products, respectively.[63] Alternatively, the redox reaction of PI_3 and $^{R}DAB^{R'}$ gives $[(^{R}DAB^{R'})P][I_3]$ (R = *t*Bu, Dipp, Mes or cHex, R′ = H; R = *p*-tolyl, R′ = Me).[64] While it has been shown that *in situ* generated "clamshell" ligand $(^{Py}BIAN)$ (Fig. 5a) adducts $(^{Py}BIAN)Pn^{III}Cl_3$ (Pn = P, As) may be reduced with cobaltocene to the corresponding N-heterocyclic chloropnictogens $(^{Py}BIAN)Pn^{I}Cl$, similar reactions with Pn = Sb and Bi species afforded black material, ^{Py}BIAN and $[Cp_2Co]Cl$.[65]

The reactivity and electrochemistry of iminopyridine complexes of Al and Ga have been studied by Berben *et al.*[66–69] and have been reviewed elsewhere.[70] It has been shown that a series of octahedral group 13 complexes of 2,6-bis{1-[(2-methoxyphenyl)imino]-benzyl}pyridine (I_2P, Fig. 5b) may be prepared that possess multiple ligand charge states: $[(I_2P^0)(I_2P^-)M]^{2+}$, $[(I_2P^-)_2M]^+$, $(I_2P^-)(I_2P^{2-})M$, $[(I_2P^{2-})_2M]^-$, and $[(I_2P^{2-})(I_2P^{3-})M]^{2-}$, and $[(I_2P^{3-})_2Al]^{3-}$ (M = Al, Ga, In).[71] This is achieved through chemical oxidation or reduction of the various complexes with $Fc(PF_6)$ or Na, respectively. Further, cyclic voltammograms of $(I_2P^-)(I_2P^{2-})M$ display reversible redox events that span ligand-based charge states from $[(I_2P^0)(I_2P^-)M]^{2+}$ up to $[(I_2P^{2-})_2M]^-$. CV scans of $(L^{NNO})TlMe_2$ (L^{NNO} = 2,4-di-*tert*-butyl-6-(3-(2,6-di-iso-propylphenylimino)butan-2-ylidene)amino phenolato; Fig. 5c) showed an irreversible reduction wave which was assigned to reduction of the ligand and accompanied by with strong adsorption of the product to the electrode surface.[72]

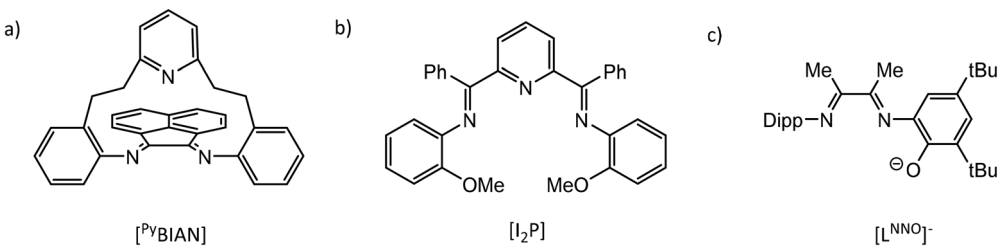

[^{Py}BIAN] [I_2P] [L^{NNO}]$^-$

Fig. 5 Structural drawings of α-diimine ligands: (a) [^{Py}BIAN], (b) [I_2P] and (c) $[L^{NNO}]^-$.

Dithiolenes (mnt), 1,2-benzenedithiolates (tdt) and 2-amidobenzenethiolates (abt)

Early polarographic studies of $[In(mnt)_3]^{3-}$, $[In(mnt)_2]^-$ and $[In(tdt)_2]^-$ (mnt = maleonitriledithiolate, tdt = 3,4-toluenedithiolate) complexes showed that these can be reversibly reduced in the steps $In^{III} \rightarrow In^{II} \rightarrow In^{I} \rightarrow In^0$, though electrochemical or chemical oxidation of these species was not studied. A series of poorly characterized antimony and bismuth-tdt and -mnt complexes have been studied similarly, with tdt complexes showing a single reversible reduction wave and mnt complexes showing two reversible reduction waves.[73] Cyclic voltammetry (CV) investigation of $[NMe_4]_2[(bdt)_2Tl^{I}_2]$ (H_2bdt = 1,2-benzenedithiol) showed an irreversible reduction wave due to reduction of Tl^+ to Tl^0 with deposition of metal on the electrode surface.[74] Further, solutions of the compound undergo colour changes upon exposure to air. CV scans of $[NEt_4][(bdt)_2Tl^{III}]$ show a single irreversible oxidation peak. More recently, it has been shown *via* CV that indium compounds (NCN)In(tdt) [NCN = 2,6-bis(dimethylaminomethyl) phenyl] and dimeric $[MeIn(tdt)(py)]_2$ undergo irreversible one-electron and two-electron electrochemical oxidations, respectively.[75] Chemical oxidation of both compounds with diiodine did not give one-electron oxidation radical products (NCN)In(tdt$^{\bullet}$)I and $[MeIn(tdt^{\bullet})(py)]_2$, as observed for indium *o*-amidophenolate (**1**) and catecholate (**11**, **12**) complexes. Instead, a spontaneous two-electron oxidation of the tdt ligand and formation of $[tdt]_n$ disulfide oligomers and $RInI_2$ (R = NCN, Me) was observed, regardless of reaction stoichiometry. CV studies of the corresponding 2-amidobenzenethiolate (abt) analogues showed two very weak oxidation peaks for (NCN)In(abt) and only background current for [MeIn(abt)(py)]. Attempts to chemically oxidize both compounds with diiodine showed no reactivity. Reaction of $[NBu_4]_2[Pb^{II}(mnt)_2]$ with organohalides (RX, where R = 1° and 2° alkyl, X = Br, I) afforded $[Pb^{II}(mnt)X]^-$ and R_2mnt, while no reaction was observed when R = 3° alkyl, aryl or X = Cl.[76] Alkylation was found to proceed faster than for $Na_2(mnt)$.

Ferrocenyl compounds (Fc)

Structural drawings of select main group metal ferrocenyl complexes are found in Fig. 6. A small number of ferrocenyl group 13 metal compounds have been synthesized and studied for their electrochemical properties *via* CV. The triel bridged [1.1] ferrocenophane complexes $(RMFc)_2$ (Fc = ferrocenyl; R = $(Me_2NCH_2)C_6H_4$ (**25**); M = Al, Ga and In) exhibit a fully reversible two-electron redox process for M = Al and a conventional step-wise redox chemistry for M = Ga, In, indicating weak interaction between the iron centres.[77,78] A similar two-electron process was observed for $[Me(py)GaFc]_2$,[78] while changing the ancillary ligand to R = $C(SiMe_3)_2SiMe_2NMe_2$ for the indium analogue results in a single irreversible oxidation wave.[79] The splitting between the oxidation potentials in bis(ferrocenyl) compounds Fc_2GaR (R = 5-Me_3Si-2-$(Me_2NCH_2)C_6H_3$ and (2-$C_5H_4N)Me_2SiCH_2$) was found to be smaller than that in the [1.1]ferroceneophane complex $(RGaFc)_2$ (R = 5-Me_3Si-2-$(Me_2NCH_2)C_6H_3$), which is accredited to differences in electrostatic interactions between the two Fe centres in each class of complex and more effective solvation of the Fe-containing moieties in Fc_2GaR.[80] A trinuclear gallium-bridged ferrocenophane with a carousel structure $[Fc_3Ga_2(py)_2]$ (**26**) shows three reversible oxidation waves with half wave potentials lower than that of ferrocene, *i.e.* it is more easily oxidized than ferrocene.[81,82]

CV of the spirocyclic [1]sila- and germaferrocenophanes $(Fc)_2M^{IV}$ (M = Si (**27a**), Ge (**27b**)) shows two one-electron oxidations, indicating Fe–Fe interactions.[83] The first oxidation is reversible in both compounds, while the second is irreversible for **27a** and reversible for **27b** at fast scan rates. [1] Germylferrocenophane compounds **28a–28c** show a reversible one-electron oxidation process with oxidation potentials significantly higher than that of ferrocene due to the electron withdrawing nature of the chloro group.[84] Compound **28d** exhibits two reversible one electron oxidation processes with the first redox process assigned to the pendant ferrocene group and the second to the ferrocenophane moiety. The bulky bis(ferrocenyl)germane compound $(Fc^{\star})_2Ge^{II}$ (Fc* = 2,5-bis(3,5-di-*tert*-butylphenyl)-1-ferrocenyl) (**29**) was shown by CV to undergo two separate two-electron oxidations.[85] Computations studies support that the first wave involves oxidation of Ge^{II} to Ge^{IV}, followed by facile intramolecular transfer from the Fe atoms in $(Fc^{\star})_2Ge^{2+}$ to afford $(Fc^{\star+})_2Ge$: as a triplet dication. The stability of $(Fc^{\star+})_2Ge$: is afforded by the steric bulk of the Fc* ligands. Compound **29** exhibits characteristic reactivity of a germylene with oxidation of Ge^{II} to Ge^{IV}.

CV of $(FcCO_2Me)_4Sn^{IV}$ (**30**) shows two sequential one-electron processes and one two-electron process.[86] This compound could also be chemically oxidized in a step-wise manner to $\mathbf{30}^+$, $\mathbf{30}^{2+}$ and $\mathbf{30}^{3+}$ using $AgSbF_6$. CV and DPV (differential pulse voltammetry) data for a series of $(FcCH_2NMe_2)_nSn^{IV}Cl_{4-n}$ (n = 1, 2, 3 or 4) (**31**) complexes shows one, two or three single electron oxidation steps for n = 1, 2 and 3, respectively. One two-electron oxidation step followed by a two one-electron oxidation steps is observed for n = 4. $(FcCH_2NMe_2)_2Sn^{II}$ shows two one-electron oxidation steps corresponding to oxidation of the ferrocenyl ligands *versus* the Sn^{II} centre.[87] CV and square wave voltammetry (SWV) for a series of multiply-$SnMe_3$ substituted ferrocenes (**32a–f**) show a reversible one-electron oxidation wave. The oxidation potential shifts to more negative values for each introduced stannyl group due their strong σ-donor and weak π-acceptor properties.[88] CV and DPV studies of the adamantly-shaped $[(FcSn)_4E_6]$ (E = S (**33a**), Se (**33b**)) and cyclic $[(FcSn)_3Te_2]$ (**34**) complexes show a single four- or six-electron reversible oxidation peak, indicating four or six equivalent and independent redox sites, respectively.[89] However, the broad oxidation peak indicates weak interaction among Fe centres, particularly for **34**, as a result of short Fe–Fe distances. The oxidation potential decreases upon replacing E = S (**33a**) with E = Se (**33b**) due to decreased electron withdrawal from the Sn centres and an increase in electron density in the ferrocenyl ligands. Alternatively, the bridged 1,1′-ferrocenyl compound $Fc(Sn(SePh)_3)_2$ (**35**) decomposes to other products upon electrochemical oxidation, most likely due to Sn–Se bond clea-

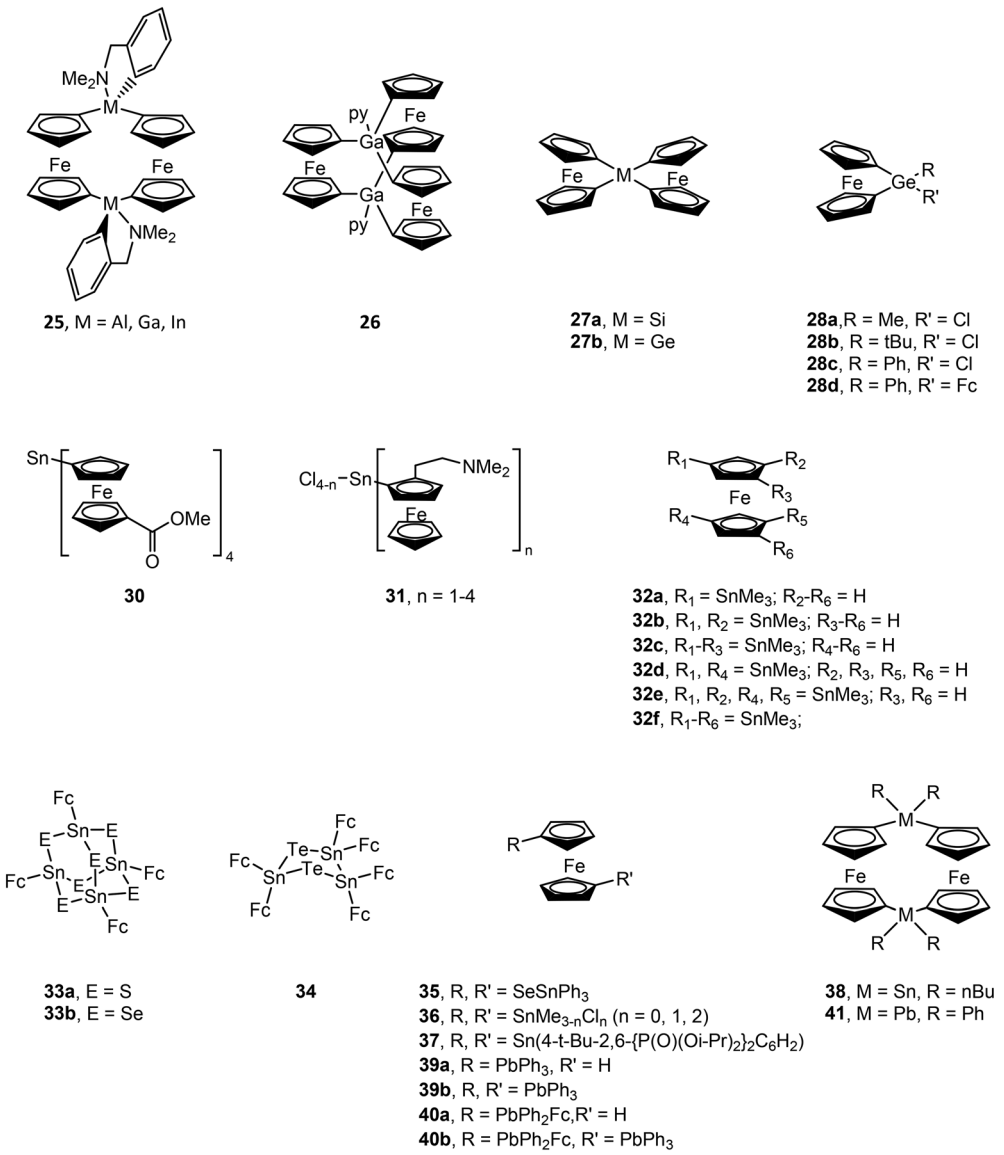

Fig. 6 Structural drawings of select main group metal ferrocenyl (Fc) compounds.

vage.[90] CV of 1,1′-bis(stannyl)ferrocenes $Fc(Sn^{IV}Me_{3-n}Cl_n)_2$ (n = 0, 1, 2) (**36**) and $Fc(Sn^{II}R)_2$ (R = 4-*t*-Bu-2,6-$\{P(O)(Oi\text{-}Pr)_2\}_2C_6H_2$) (**37**) show reversible one-electron oxidations,[91,92] as does 1,1′-bis(diphenylstibino)ferrocene.[93] Polarographic measurements of the [1.1]stannylferrocenophane ($(n\text{-}Bu)_2SnFc)_2$ (**38**) shows two reversible one-electron oxidation waves.[94] Oxidation potentials have also been obtained by CV for ferrocenyl lead compounds Ph_3PbFc (**39a**), $(Ph_3Pb)_2Fc$ (**39b**), Ph_2PbFc_2 (**40a**) and $(Ph_3Pb)Fc(Ph_2Pb)Fc$ (**40b**) and lead [1.1]ferrocenophane $(Ph_2PbFc)_2$ (**41**).[95] All compounds show separate one-electron oxidation wave for each Fc ligand. The first oxidation is at slightly higher potentials *versus* ferrocene for all compounds except for **40a** where the first oxidation is at a slightly lower potential.

The 1,2-bis(ferrocenyl)dibismuthene Fc*M═MFc* (Fc* = 2,5-(3,5-dimethylphenyl)-1-ferrocenyl; M = Sb, Bi) features two bulky Fc* ligands bridged by a M═M π-spacer.[96] CV shows three reversible one-electron oxidation couples, corresponding to oxidation of each of the Fc* ligands followed by the M═M double bond. This suggests that the trication is stabilized by the ferrocenyl groups. CV scans of the 1,2-bis(ferrocenyl)digermene (*E*)-Trip(Fc)Ge═Ge(Fc)Trip (Trip = 2,4,6-triisopropylphenyl) show a two-step reversible redox couple, suggesting coupling of the two ferrocenyl moieties through the Ge═Ge π bond.[97] Although ferrocene may be chemically oxidized to give the ferrocenium cation,[98] no studies involving chemical oxidation of ferrocenyl indium or bismuth compounds have been reported.

Porphyrinates (Por)

Structural drawings of substituted porphyrinato ligands 5,10,15,20-tetraphenylporphyrinato (TPP), 5,10,15,20-tetra

(pentafluorophenyl)porphyrinato (TPFP), 5,10,15,20-tetraferrocenylporphyrinato (TFcP), tetrakis[3,5-bis(trifluoromethyl) phenyl]porphyrinato (TAr^{F}P), 5,10,15,20-tetra-*p*-tolylporphyrinato (TTP), 5,10,15,20-tetramesitylporphyrinato (TMesP), 2,3,7,8,12,13,17,18-octaethylporphyrinato (OEP) and 2,3,12,13-tetrabromo-5,10,15,20-tetraphenylporphyrinato (Br_4TPP) are found in Fig. 7. CV data has been reported for series of main group metal porphyrin complexes (TPP)AlR and (OEP)AlR (R = Me, *n*Bu, Ph, C_6F_4H)[99] and show one irreversible one-electron oxidation wave followed by two reversible one-electron oxidation waves. The first corresponds to the formation of $[(TPP/OEP)AlR]^{\bullet+}$ followed by loss of R$^\bullet$ to give $[(TPP/OEP)Al]^+$. The second and third oxidation peaks correspond to oxidation of the porphyrin ligand. (TPP)MMe and (OEP)MMe (M = Ga, In) show similar redox behavior. However, cleavage of the M–Me does not occur for the M = Tl complexes and only the two reversible oxidation waves are observed. Al(TPP)Cl and Al(Por)Cl, react with Na/Hg in THF to yield the stable radicals $[Al(TPP)(THF)_2]^\bullet$ and $[Al(Por)(THF)_2]^\bullet$, respectively.[100] Both are monomeric in solution with the unpaired electron delocalized throughout the ring system.

(TPFP)GaCl (**42**) was shown to be a highly active and stable post-transition metal-based electrocatalyst for the hydrogen evolution reaction (HER).[101] Electrochemical and spectroscopic studies in acidic media show that both the first and second reduction events of **42** are ligand-centered. The two-electron reduced form then reacts with a proton to give a Ga^{III}–H species, which subsequently undergoes protonolysis to produce H_2. Photolysis of (TPP)Ga^{III}($(CH_2)_4CH{=}CH_2$) (**43**) in benzene solution results in isomerization to form (TPP)Ga^{III}($CH_2CH(CH_2)_4$) as a result of homolytic cleavage of the Ga–C bond followed by cyclization of the 5-hexenyl radical.[102] When the photolysis of (TPP)Ga^{III}(C_2H_5) is carried out in the presence of dioxygen, the alky radical is trapped to form a alkylperoxy radical which recombines with the gallium radical to produce the peroxide (TPP)Ga^{III}(OOC_2H_5). The formation of (TPP)Ga^{III}($OO(CH_2)_4CH{=}CH_2$) during the photolysis of **43** in the presence of dioxygen suggests that reaction with dioxygen occurs faster that cyclization.

CV, DPV, and SWV studies of (TFcP)InX (X = Cl, OH, Fc) show reversible oxidation of all four ferrocene substituents, and an irreversible porphyrin-centred oxidation at high positive potentials.[103] The X = Fc compound shows a fifth reversible oxidation peak at lower potentials that was assigned to the axial In-ferrocenyl ligand using characteristic IVTC bands in the UV-vis-NIR spectra. These compounds were also chemically oxidized to the corresponding monocations using silver(I) triflate or dichloro-5,6-dicyanobenzoquinone (DDQ). Again, UV-vis-NIR spectroscopy was used to confirm oxidation of the axial In-ferrocenyl ligand.

The aromatic complex (TPP)Ge^{II} (**44**) is converted to antiaromatic (TPP)Ge^{IV}$(py)_2$ (**45**) in pyridine solution.[104] The reaction is reversed in benzene solution where pyridine dissociates from **45** to reform **44**. This represents an unusual example of an oxidation-state change in a metal induced by coordination of a dative ligand. The complex (TAr^{F}P)Ge^{II}, which possesses a more electron withdrawing ligand, behaves similarly but favours the antiaromatic (TAr^{F}P)Ge^{IV}$(py)_2$ product. Experimental observations and DFT studies indicate that formation of (TPP)M^{IV}$(py)_2$ from (TPP)M^{II} in pyridine is most favourable for M = Si, borderline for M = Ge and unfavourable for M = Sn.

CV and DPV experiments on (TPP)Sn^{IV}$(Fc)_2$ complexes reveal three reversible oxidation processes and two reversible reduction processes.[105] The first two closely spaced oxidations were assigned to single-electron ferrocene-centered processes, while the third oxidation and both reduction couples are porphyrin core-centered single-electron processes. Both ferrocene substituents are oxidized at lower potentials compared to ferrocene. Chemical oxidation revealed two key processes associated with consecutive oxidation of the axial ferrocene substituents. The CV and SWV voltammograms of (TPP)Sn^{IV}$(FcCOO)_2$ exhibit a single two-electron oxidative wave corresponding to simultaneous oxidation of the ferrocenecar-

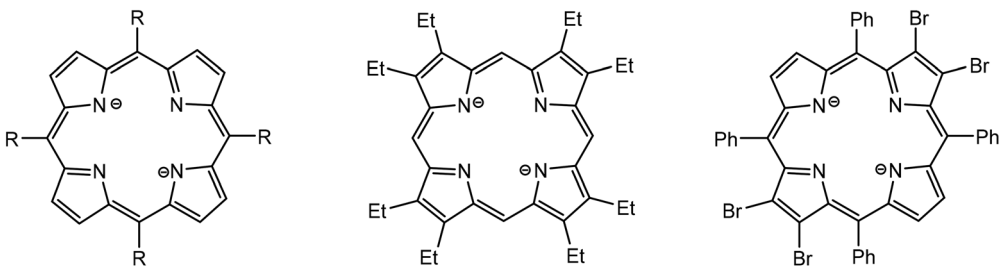

TPP, R = Ph
TPFP, R = C_6F_5
TFcP, R = Fc
TAr^{F}P, R = 3,5-$(CF_3)_2C_6H_3$
TTP, R = 4-MeC_6H_4
TMesP, R = 2,4,6-$Me_3C_6H_2$

OEP

Br_4TPP

Fig. 7 Structural drawings of porphyrinato (Por) ligands.

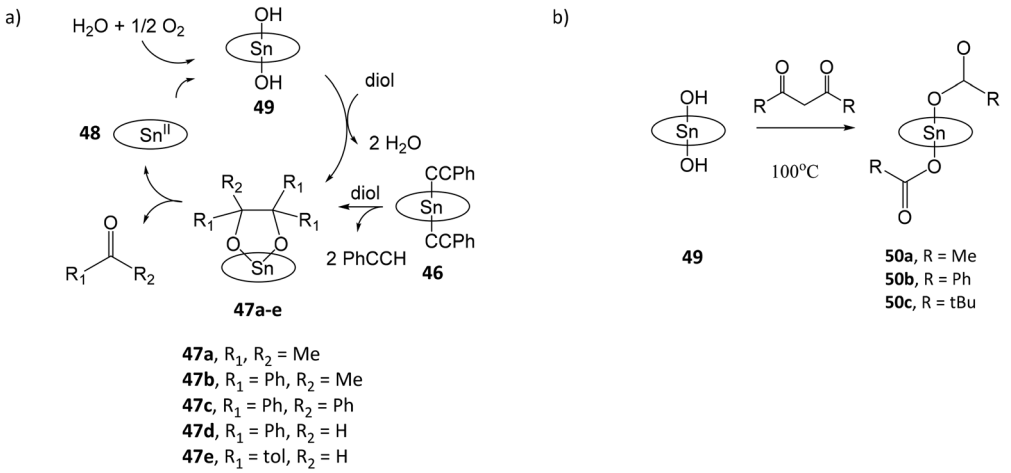

Fig. 8 (a) Catalytic cycle for the oxidative cleavage of vicinal diols by tin porphyrin complexes; (b) reaction of (TTP)$Sn^{IV}(OH)_2$ (**49**) with β-diketones to form dicarboxylato tin(IV) porphyrin complexes (**50a–c**).

boxylato ligands. Two reversible TPP ligand reduction waves were also observed.[106] CV studies of the complexes of (Br_4TPP)SnX (X = Cl, OH, OPh, *p*-(NO_2)C_6H_4O) show two reversible reduction peaks, which are shifted to lower potentials *versus* non-brominated analogues due to the electron withdrawing effect of the β-bromine atoms.[107]

Tin porphyrin complexes were found to promote the oxidative cleavage of vicinal diols (Fig. 8a).[108] Treatment of (TTP)Sn^{IV}(C≡CPh)$_2$ (**46**) or (TTP)Sn^{IV}(NHtolyl)$_2$ with pinacol and 2,3-diphenylbutane-2,3-diol afforded diolato complexes (TTP)Sn^{IV}[$OC(Me)_2C(Me)_2O$] (**47a**) and (TTP)Sn^{IV}[OC(Ph)(Me)C(Ph)(Me)O] (**47b**), respectively. Both complexes spontaneously undergo C–C cleavage reactions to give (TTP)Sn^{II} (**48**) and ketones O=CMe_2 and O=CMe(Ph), respectively. In the presence of moist air, **48** is oxidized by dioxygen to (TTP)$Sn^{IV}(OH)_2$ (**49**), which reacts with vicinal diols to reform (TTP)Sn^{IV}[$OC(R)_2C(R)_2O$] (**47**), thus completing the catalytic cycle. The oxidation state of the metal or TTP ligand in **48** is not confirmed in the study. In a subsequent study, the reaction of **49** with β-diketones acetylacetone, dibenzoylmethane, 1-phenylbutane-1,3-dione or 4,4-dimethyl-1-phenylpentane-1,3-dione afforded dicarboxylato tin(IV) porphyrin complexes (TPP)$Sn^{IV}(O_2CR)_2$ (R = Me (**50a**), Ph (**50b**), *t*-Bu (**50c**)) and ketonic compounds due to the C–C bond cleavage of β-diketones (Fig. 8b).[109] The proposed mechanism involves nucleophilic attack of the OH ligands of **49**, and a four-centred intermediate involving C–C and O–H bond cleavage and C–O and C–H bond formation. The enhanced nucleophilicity of hydroxo-ligands capable of the C–C bond cleavage of β-diketones is attributed to the electron-donating influence of porphyrin ligand to stabilize the high-valent Sn^{IV} center and increase the basicity of the hydroxo-ligands.

CV studies of (L)BiX (L = TPP, TTP, TMesP or OEP; X = SO_3CF_3, NO_3) shows two reversible oxidation waves for each compound.[110] UV-visible spectra of oxidized species confirm that only the porphyrin ligand is oxidized and there that is no evidence for oxidation of Bi(III) to Bi(V) in the complex. Oxidation potentials were found to vary little as a function of the counterion or solvent.

Conclusions and outlook

The reactivity and electrochemical studies presented herein highlight the potentially rich and diverse chemistry of main group metal compounds of incorporating redox-active ligands. For example, the oxidation of metal *o*-amidophenolate $(^{R}AP)^{2-}$ and catecholate $(^{R}Cat)^{2-}$ compounds to produce stable *o*-iminosemiquinone $(^{R}ISQ^{\bullet})^{-}$ and *o*-semiquinone $(^{R}SQ^{\bullet})^{-}$ compounds demonstrates the ability of these ligands to facilitate these reactions by acting as sources of electrons. Further, this reactivity can be tuned through choice of ligand substituents, which affects the redox potential of the ligand. The reversible addition of dioxygen to antimony(V) *o*-amidophenolates and catecholates and the reversible addition of alkynes to $(^{R}BIAN)^{2-}$ supported digallanes provide examples of the corresponding reductive elimination reaction required for catalytic applications. The latter was further exploited to facilitate the catalytic hydroamination of phenylacetylenes with aniline. In both cases, bonding of the substrate was to both the metal center and the ligand, highlighting the potential for non-innocent participation of the redox-active ligand in chemical transformations. The non-innocent ligand behavior of aluminum bis(imino)pyridine compounds has been exploited by Berben *et al.* to mediate proton transfer for dehydrogenation catalysis. Alternatively, the catalytic oxidative C–C bond cleavage of visceral diols by a tin(IV) porphyrin complex does not involve direct participation by the porphyrin ligand, which primarily serves to promote oxidative addition and reductive elimination reactions at the tin center. Finally, the potential for reversible intramolecular electron transfer has also been shown in the redox isomerism observed in homoleptic bis(*o*-amidopheno-

lato)tin(IV)/bis(*o*-iminosemiquinolato)tin(II) compounds and during electrochemical oxidation of mixed ligand catecholato/ferrocenyl tin(IV) compounds and ferrocenyl germanium(II) compounds.

Despite these observations, information on the redox properties and reactivity of redox-active ligand compounds of main group metals, particularly those of indium and bismuth, remains relatively sparse. For example, the facile oxidation and spontaneous disproportionation reactions observed for indium *o*-amidophenolate and catecholate complexes demonstrate a high degree of reactivity. However, the chemical and electrochemical reversibility of these reactions has not yet been studied. Further, reactivity with a scope of substrates, including reactions with organohalides, small molecules and symmetric and asymmetric unsaturated species, has not been demonstrated. The spontaneous two-electron chemical oxidation of indium 3,4-toluenedithiolate species to yield oligomeric disulfides *versus* the controlled one-electron chemical oxidation of indium *o*-amidophenolates and catecholates shows the potential for varying reactivity with the choice of redox-active ligand. The ligand centered electrochemically reversible oxidation of ferrocenyl- and porphyrinato-indium and bismuth species suggest possible reversible chemical reactivity, while tunability of redox potentials is possible though modification of ligand substituents. Further, the synthesis of mixed redox active ligand systems leaves potential for expanding the scope of reactivity for these species.

The studies discussed herein confirm the ability of main group metal compounds of redox-active ligands to undergo "oxidative addition" type reactions to afford isolable species. However, it remains that only a very small number of these chemical reactions have been shown to be reversible. Therefore, the current challenge in the field is the identification of new reversible chemical reactions that also feature corresponding "reductive elimination" processes. This will ultimately require systematic studies involving informed selection of main group metal, redox-active ligand, substituents and substrate. In the quest to establish the potential utility of main group metal compounds in catalytic redox processes, the chemical reactivity and electrochemical properties of compounds containing redox-active ligands is an intriguing avenue of inquiry and one that should be fully explored.

Conflicts of interest

There are no conflicts to declare.

Acknowledgements

Natural Sciences and Engineering Research Council of Canada (RGPIN-2019-05965), the New Brunswick Innovation Foundation, the Canadian Foundation for Innovation (Project No. 9211) and Mount Allison University are thanked for financial support.

References

1 P. P. Power, *Nature*, 2010, **463**, 171–177.
2 C. Weetman and S. Inoue, *ChemCatChem*, 2018, **10**, 4213–4228.
3 M.-A. Légaré, C. Pranckevicius and H. Braunschweig, *Chem. Rev.*, 2019, **119**, 8231–8261.
4 T. Chu and G. I. Nikonov, *Chem. Rev.*, 2018, **118**, 3608–3680.
5 O. Planas, F. Wang, M. Leutzsch and J. Cornella, *Science*, 2020, **367**, 313–317.
6 O. Planas, V. Peciukenas and J. Cornella, *J. Am. Chem. Soc.*, 2020, **142**, 11382–11387.
7 H. W. Moon and J. Cornella, *ACS Catal.*, 2022, **12**, 1382–1393.
8 W. Kaim, *Eur. J. Inorg. Chem.*, 2012, **2012**, 343–348.
9 O. R. Luca and R. H. Crabtree, *Chem. Soc. Rev.*, 2013, **42**, 1440–1459.
10 T. Fogeron, T. K. Todorova, J.-P. Porcher, M. Gomez-Mingot, L.-M. Chamoreau, C. Mellot-Draznieks, Y. Li and M. Fontecave, *ACS Catal.*, 2018, **8**, 2030–2038.
11 V. K. K. Praneeth, M. R. Ringenberg and T. R. Ward, *Angew. Chem., Int. Ed.*, 2012, **51**, 10228–10234.
12 V. Lyaskovskyy and B. de Bruin, *ACS Catal.*, 2012, **2**, 270–279.
13 P. J. Chirik and K. Wieghardt, *Science*, 2010, **327**, 794–795.
14 D. L. J. Broere, R. Plessius and J. I. van der Vlugt, *Chem. Soc. Rev.*, 2015, **44**, 6886–6915.
15 J. I. van der Vlugt, *Chem. – Eur. J.*, 2019, **25**, 2651–2662.
16 B. Garreau-de Bonneval, K. I. Moineau-Chane Ching, F. Alary, T.-T. Bui and L. Valade, *Coord. Chem. Rev.*, 2010, **254**, 1457–1467.
17 R. O. Fields, J. H. Waters and T. J. Bergendahl, *Inorg. Chem.*, 1971, **10**, 2808–2810.
18 D. G. Tuck and M. K. Yang, *J. Chem. Soc. A*, 1971, 214–219.
19 I. V. Ershova and A. V. Piskunov, *Russ. J. Coord. Chem.*, 2020, **46**, 154–177.
20 A. V. Piskunov, I. V. Ershova and G. K. Fukin, *Russ. Chem. Bull.*, 2014, **63**, 916–922.
21 A. V. Piskunov, I. N. Mescheryakova, A. S. Bogomyakov, G. V. Romanenko, V. K. Cherkasov and G. A. Abakumov, *Inorg. Chem. Commun.*, 2009, **12**, 1067–1070.
22 A. V. Piskunov, I. N. Mescheryakova, G. K. Fukin, V. K. Cherkasov and G. A. Abakumov, *New J. Chem.*, 2010, **34**, 1746–1750.
23 A. V. Piskunov, I. N. Meshcheryakova, I. V. Ershova, A. S. Bogomyakov, A. V. Cherkasov and G. K. Fukin, *RSC Adv.*, 2014, **4**, 42494–42505.
24 I. V. Ershova, A. S. Bogomyakov, G. K. Fukin and A. V. Piskunov, *Eur. J. Inorg. Chem.*, 2019, **2019**, 938–948.
25 A. V. Piskunov, I. N. Meshcheryakova, G. K. Fukin, A. S. Shavyrin, V. K. Cherkasov and G. A. Abakumov, *Dalton Trans.*, 2013, **42**, 10533–10539.
26 A. V. Piskunov, I. V. Ershova, G. K. Fukin and A. S. Shavyrin, *Inorg. Chem. Commun.*, 2013, **38**, 127–130.
27 P. Chaudhuri, E. Bill, R. Wagner, U. Pieper, B. Biswas and T. Weyhermüller, *Inorg. Chem.*, 2008, **47**, 5549–5551.

28 K. V. Arsenyeva, A. V. Klimashevskaya, M. A. Zherebtsov, M. G. Chegerev, A. V. Cherkasov, I. A. Yakushev and A. V. Piskunov, *Russ. J. Coord. Chem.*, 2022, **48**, 464–477.
29 K. V. Arsenyeva, K. I. Pashanova, O. Y. Trofimova, I. V. Ershova, M. G. Chegerev, A. A. Starikova, A. V. Cherkasov, M. A. Syroeshkin, A. Y. Kozmenkova and A. V. Piskunov, *New J. Chem.*, 2021, **45**, 11758–11767.
30 A. V. Piskunov, K. V. Tsys, M. G. Chegerev and A. V. Cherkasov, *Russ. J. Coord. Chem.*, 2019, **45**, 626–636.
31 M. G. Chegerev, A. V. Piskunov, A. A. Starikova, S. P. Kubrin, G. K. Fukin, V. K. Cherkasov and G. A. Abakumov, *Eur. J. Inorg. Chem.*, 2018, **2018**, 1087–1092.
32 A. V. Piskunov, I. N. Mescheryakova, G. K. Fukin, A. S. Bogomyakov, G. V. Romanenko, V. K. Cherkasov and G. A. Abakumov, *Heteroat. Chem.*, 2009, **20**, 332–340.
33 K. V. Tsys, M. G. Chegerev, G. K. Fukin and A. V. Piskunov, *Mendeleev Commun.*, 2018, **28**, 527–529.
34 A. V. Piskunov, I. N. Mescheryakova, G. K. Fukin, E. V. Baranov, M. Hummert, A. S. Shavyrin, V. K. Cherkasov and G. A. Abakumov, *Chem. – Eur. J.*, 2008, **14**, 10085–10093.
35 A. V. Piskunov, M. G. Chegerev and G. K. Fukin, *J. Organomet. Chem.*, 2016, **803**, 51–57.
36 M. G. Chegerev, A. V. Piskunov, A. V. Maleeva, G. K. Fukin and G. A. Abakumov, *Eur. J. Inorg. Chem.*, 2016, **2016**, 3813–3821.
37 S. V. Baryshnikova, A. I. Poddel'sky, E. V. Bellan, I. V. Smolyaninov, A. V. Cherkasov, G. K. Fukin, N. T. Berberova, V. K. Cherkasov and G. A. Abakumov, *Inorg. Chem.*, 2020, **59**, 6774–6784.
38 G. K. Fukin, E. V. Baranov, A. I. Poddel'sky, V. K. Cherkasov and G. A. Abakumov, *ChemPhysChem*, 2012, **13**, 3773–3776.
39 G. A. Abakumov, A. I. Poddel'sky, E. V. Grunova, V. K. Cherkasov, G. K. Fukin, Y. A. Kurskii and L. G. Abakumova, *Angew. Chem., Int. Ed.*, 2005, **44**, 2767–2771.
40 A. I. Poddel'sky, Y. A. Kurskii, A. V. Piskunov, N. V. Somov, V. K. Cherkasov and G. A. Abakumov, *Appl. Organomet. Chem.*, 2011, **25**, 180–189.
41 A. I. Poddel'sky, N. N. Vavilina, N. V. Somov, V. K. Cherkasov and G. A. Abakumov, *J. Organomet. Chem.*, 2009, **694**, 3462–3469.
42 V. K. Cherkasov, G. A. Abakumov, E. V. Grunova, A. I. Poddel'sky, G. K. Fukin, E. V. Baranov, Y. V. Kurskii and L. G. Abakumova, *Chem. – Eur. J.*, 2006, **12**, 3916–3927.
43 P. Chaudhuri, M. Hess, K. Hildenbrand, E. Bill, T. Weyhermüller and K. Wieghardt, *Inorg. Chem.*, 1999, **38**, 2781–2790.
44 G. Szigethy and A. F. Heyduk, *Dalton Trans.*, 2012, **41**, 8144–8152.
45 U. Beckmann, E. Bill, T. Weyhermüller and K. Wieghardt, *Eur. J. Inorg. Chem.*, 2003, **2003**, 1768–1777.
46 A. V. Piskunov, A. V. Maleeva, I. N. Meshcheryakova and G. K. Fukin, *Russ. J. Coord. Chem.*, 2013, **39**, 245–256.
47 A. I. Poddel'sky, I. V. Smolyaninov, Y. A. Kurskii, G. K. Fukin, N. T. Berberova, V. K. Cherkasov and G. A. Abakumov, *J. Organomet. Chem.*, 2010, **695**, 1215–1224.
48 A. I. Poddel'sky, I. V. Smolyaninov, N. V. Somov, N. T. Berberova, V. K. Cherkasov and G. A. Abakumov, *J. Organomet. Chem.*, 2010, **695**, 530–536.
49 V. K. Cherkasov, E. V. Grunova, A. I. Poddel'sky, G. K. Fukin, Y. A. Kurskii, L. G. Abakumova and G. A. Abakumov, *J. Organomet. Chem.*, 2005, **690**, 1273–1281.
50 Y. Zhao, Y. Liu, L. Yang, J.-G. Yu, S. Li, B. Wu and X.-J. Yang, *Chem. – Eur. J.*, 2012, **18**, 6022–6030.
51 I. L. Fedushkin, A. A. Skatova, V. A. Dodonov, V. A. Chudakova, N. L. Bazyakina, A. V. Piskunov, S. V. Demeshko and G. K. Fukin, *Inorg. Chem.*, 2014, **53**, 5159–5170.
52 I. L. Fedushkin, A. S. Nikipelov, A. A. Skatova, O. V. Maslova, A. N. Lukoyanov, G. K. Fukin and A. V. Cherkasov, *Eur. J. Inorg. Chem.*, 2009, **2009**, 3742–3749.
53 I. L. Fedushkin, A. S. Nikipelov and K. A. Lyssenko, *J. Am. Chem. Soc.*, 2010, **132**, 7874–7875.
54 I. L. Fedushkin, A. S. Nikipelov, A. G. Morozov, A. A. Skatova, A. V. Cherkasov and G. A. Abakumov, *Chem. – Eur. J.*, 2012, **18**, 255–266.
55 C. J. Allan, B. F. T. Cooper, H. J. Cowley, J. M. Rawson and C. L. B. Macdonald, *Chem. – Eur. J.*, 2013, **19**, 14470–14483.
56 R. J. Baker, R. D. Farley, C. Jones, M. Kloth and D. M. Murphy, *Chem. Commun.*, 2002, 1196–1197.
57 R. J. Baker, R. D. Farley, C. Jones, D. P. Mills, M. Kloth and D. M. Murphy, *Chem. – Eur. J.*, 2005, **11**, 2972–2982.
58 H. Rojas-Sáenz, G. V. Suárez-Moreno, I. Ramos-García, A. M. Duarte-Hernández, E. Mijangos, A. Peña-Hueso, R. Contreras and A. Flores-Parra, *New J. Chem.*, 2013, **38**, 391–405.
59 J. Wang, R. Ganguly, L. Yongxin, J. Díaz, H. S. Soo and F. García, *Dalton Trans.*, 2016, **45**, 7941–7946.
60 J. Wang, R. Ganguly, L. Yongxin, J. Díaz, H. S. Soo and F. García, *Inorg. Chem.*, 2017, **56**, 7811–7820.
61 V. A. Dodonov, O. A. Kushnerova, D. A. Razborov, E. V. Baranov, E. A. Ulivanova, A. N. Lukoyanov and I. L. Fedushkin, *Russ. Chem. Bull.*, 2022, **71**, 322–329.
62 G. Reeske, C. R. Hoberg, N. J. Hill and A. H. Cowley, *J. Am. Chem. Soc.*, 2006, **128**, 2800–2801.
63 J. W. Dube, G. J. Farrar, E. L. Norton, K. L. S. Szekely, B. F. T. Cooper and C. L. B. Macdonald, *Organometallics*, 2009, **28**, 4377–4384.
64 G. Reeske and A. H. Cowley, *Inorg. Chem.*, 2007, **46**, 1426–1430.
65 A. L. Brazeau, N. D. Jones and P. J. Ragogna, *Dalton Trans.*, 2012, **41**, 7890–7896.
66 T. W. Myers and L. A. Berben, *Inorg. Chem.*, 2012, **51**, 1480–1488.
67 T. M. Bass, C. R. Carr, T. J. Sherbow, J. C. Fettinger and L. A. Berben, *Inorg. Chem.*, 2020, **59**, 13517–13523.

68 T. J. Sherbow, L. W. T. Parsons, N. A. Phan, J. C. Fettinger and L. A. Berben, *Inorg. Chem.*, 2020, **59**, 17614–17619.
69 A. Arnold, T. J. Sherbow, A. M. Bohanon, R. I. Sayler, R. D. Britt, A. M. Smith, J. C. Fettinger and L. A. Berben, *Chem. Sci.*, 2021, **12**, 675–682.
70 L. A. Berben, *Chem. – Eur. J.*, 2015, **21**, 2734–2742.
71 A. Arnold, T. J. Sherbow, R. I. Sayler, R. D. Britt, E. J. Thompson, M. T. Muñoz, J. C. Fettinger and L. A. Berben, *J. Am. Chem. Soc.*, 2019, **141**, 15792–15803.
72 E. N. Egorova, N. O. Druzhkov, A. S. Shavyrin, A. V. Cherkasov, G. A. Abakumov and A. Y. Fedorov, *RSC Adv.*, 2015, **5**, 19362–19367.
73 G. Hunter, *J. Chem. Soc., Dalton Trans.*, 1972, 1496–1498.
74 B. E. Bosch, M. Eisenhawer, B. Kersting, K. Kirschbaum, B. Krebs and D. M. Giolando, *Inorg. Chem.*, 1996, **35**, 6599–6605.
75 G. G. Briand, T. George, G. A. MacNeil, J. D. Masuda, B. J. MacLean, M. W. R. Mosher, G. M. Sandala, P. Srinivasan, A. H. Stockli, R. L. Vanderkloet and C. J. Walsby, *Eur. J. Inorg. Chem.*, 2023, **26**, e202200542.
76 C. W. Allen, D. E. Lutes, E. J. Durhan and E. S. Bretschneider, *Inorg. Chim. Acta*, 1977, **21**, 277–279.
77 J. A. Schachner, G. A. Orlowski, J. W. Quail, H.-B. Kraatz and J. Müller, *Inorg. Chem.*, 2006, **45**, 454–459.
78 A. Althoff, P. Jutzi, N. Lenze, B. Neumann, A. Stammler and H.-G. Stammler, *Organometallics*, 2003, **22**, 2766–2774.
79 J. A. Schachner, C. L. Lund, I. J. Burgess, J. W. Quail, G. Schatte and J. Müller, *Organometallics*, 2008, **27**, 4703–4710.
80 B. Bagh, N. C. Breit, K. Harms, G. Schatte, I. J. Burgess, H. Braunschweig and J. Müller, *Inorg. Chem.*, 2012, **51**, 11155–11167.
81 P. Jutzi, N. Lenze, B. Neumann and H.-G. Stammler, *Angew. Chem., Int. Ed.*, 2001, **40**, 1423–1427.
82 A. Althoff, D. Eisner, P. Jutzi, N. Lenze, B. Neumann, W. W. Schoeller and H.-G. Stammler, *Chem. – Eur. J.*, 2006, **12**, 5471–5480.
83 M. J. MacLachlan, A. J. Lough, W. E. Geiger and I. Manners, *Organometallics*, 1998, **17**, 1873–1883.
84 M. Castruita, F. Cervantes-Lee, J. S. Mahmoud, Y. Zhang and K. H. Pannell, *J. Organomet. Chem.*, 2001, **637–639**, 664–668.
85 Y. Suzuki, T. Sasamori, J.-D. Guo and N. Tokitoh, *Chem. – Eur. J.*, 2018, **24**, 364–368.
86 D. Siebler, C. Förster, T. Gasi and K. Heinze, *Chem. Commun.*, 2010, **46**, 4490–4492.
87 K. Jacob, N. Seidel, F. Voigt, A. Fischer, C. Pietzsch, J. Holecek, A. Lycka, M. Fontani, E. Grigiotti and P. Zanello, *J. Prakt. Chem.*, 2000, **342**, 574–584.
88 N. Lenze, B. Neumann, A. Salmon, A. Stammler, H.-G. Stammler and P. Jutzi, *J. Organomet. Chem.*, 2001, **619**, 74–87.
89 Z. You, J. Bergunde, B. Gerke, R. Pöttgen and S. Dehnen, *Inorg. Chem.*, 2014, **53**, 12512–12518.
90 H. P. Nayek, G. Hilt and S. Dehnen, *Eur. J. Inorg. Chem.*, 2009, **2009**, 4205–4208.
91 M. Herberhold, W. Milius, U. Steffl, K. Vitzithum, B. Wrackmeyer, R. H. Herber, M. Fontani and P. Zanello, *Eur. J. Inorg. Chem.*, 1999, **1999**, 145–151.
92 M. Henn, M. Schürmann, B. Mahieu, P. Zanello, A. Cinquantini and K. Jurkschat, *J. Organomet. Chem.*, 2006, **691**, 1560–1572.
93 J. Schulz, J. Antala, I. Císařová and P. Štěpnička, *Dalton Trans.*, 2023, **52**, 1198–1211.
94 T.-Y. Dong, M.-Y. Hwang, Y. Wen and W.-S. Hwang, *J. Organomet. Chem.*, 1990, **391**, 377–385.
95 G. Utri, K.-E. Schwarzhans and G. M. Allmaier, *Z. Naturforsch., B: J. Chem. Sci.*, 1990, **45**, 755–762.
96 M. Sakagami, T. Sasamori, H. Sakai, Y. Furukawa and N. Tokitoh, *Chem. – Asian J.*, 2013, **8**, 690–693.
97 T. Sasamori, H. Miyamoto, H. Sakai, Y. Furukawa and N. Tokitoh, *Organometallics*, 2012, **31**, 3904–3910.
98 H. B. Gray, D. N. Hendrickson and Y. S. Sohn, *Inorg. Chem.*, 1971, **10**, 1559–1563.
99 R. Guilard, A. Zrineh, A. Tabard, A. Endo, B. C. Han, C. Lecomte, M. Souhassou, A. Habbou, M. Ferhat and K. M. Kadish, *Inorg. Chem.*, 1990, **29**, 4476–4482.
100 J. A. Cissell, T. P. Vaid and A. L. Rheingold, *Inorg. Chem.*, 2006, **45**, 2367–2369.
101 N. Wang, H. Lei, Z. Zhang, J. Li, W. Zhang and R. Cao, *Chem. Sci.*, 2019, **10**, 2308–2314.
102 A. L. Balch, R. L. Hart and S. Parkin, *Inorg. Chim. Acta*, 1993, **205**, 137–143.
103 S. J. Dammer, P. V. Solntsev, J. R. Sabin and V. N. Nemykin, *Inorg. Chem.*, 2013, **52**, 9496–9510.
104 J. A. Cissell, T. P. Vaid and G. P. A. Yap, *J. Am. Chem. Soc.*, 2007, **129**, 7841–7847.
105 P. V. Solntsev, J. R. Sabin, S. J. Dammer, N. N. Gerasimchuk and V. N. Nemykin, *Chem. Commun.*, 2010, **46**, 6581–6583.
106 H. J. Kim, W. S. Jeon, J. H. Lim, C. S. Hong and H.-J. Kim, *Polyhedron*, 2007, **26**, 2517–2522.
107 M. Ravikumar, A. Kathiravan, A. Neels and E. M. Mothi, *Eur. J. Inorg. Chem.*, 2018, **2018**, 3868–3877.
108 G. Du, A. Ellern and L. K. Woo, *Inorg. Chem.*, 2004, **43**, 2379–2386.
109 A. P. Singh, B. B. Park and H.-J. Kim, *Tetrahedron Lett.*, 2012, **53**, 6456–6459.
110 L. Michaudet, D. Fasseur, R. Guilard, Z. Ou, K. M. Kadish, S. Dahaoui and C. Lecomte, *J. Porphyrins Phthalocyanines*, 2000, **4**, 261–270.